Development 135, 3567-3576 (2008) doi:10.1242/dev.028076

An essential role for frizzled 5 in mammalian ocular development

Chunqiao Liu[1] and Jeremy Nathans[1,2,3,4,*]

Microphthalmia, coloboma and persistent fetal vasculature within the vitreous cavity are among the most common human congenital ocular anomalies, and each has been associated with a variety of genetic disorders. Here we show that, in the mouse, loss of frizzled 5 (Fz5) – a putative Wnt receptor expressed in the eye field, optic cup and retina – causes all of these defects with high penetrance. In the developing *Fz5*$^{-/-}$ eye, the sequence of defects, in order of appearance, is: increased cell death in the ventral retina, delayed and/or incomplete closure of the ventral fissure, an excess of mesenchymal cells in the vitreous cavity, an excess of retinal astrocyte precursors and mature astrocytes, and persistence of the hyaloid vasculature in association with a large number of pigment cells. *Fz5*$^{-/-}$ mice also exhibit a late-onset progressive retinal degeneration by ~6 months of age, which might be related to the expression of Fz5 in Müller glia in the adult retina. These results demonstrate a central role for frizzled signaling in mammalian eye development and are likely to be relevant to the etiology of congenital human ocular anomalies.

KEY WORDS: Coloboma, frizzled 5 (Fz5; Fzd5), Microphthalmia, Optic fissure, PFV, Retinal degeneration

INTRODUCTION

Eye development is perturbed in a wide variety of syndromic and non-syndromic disorders. Among the more common defects are microphthalmia, coloboma (congenital ocular fissure) and persistent fetal vasculature (PFV) within the vitreous cavity. Insights into the molecular origins of these ocular defects have come primarily from studies of laboratory animals, and of genetically altered mice in particular.

Microphthalmia, and its more extreme variant anophthalmia, are associated with a variety of monogenic, chromosomal and environmental causes (Verma and Fitzpatrick, 2007). The first category includes mutations in transcription factor genes, including *Pax6*, *Chx10* (*Vsx2*), *Sox2* and *Otx2* (Horsford et al., 2001). A coloboma arises from incomplete closure of the ventral fissure, a transient opening in the embryonic eyecup that extends anteriorly from the future optic disc at the junction between the optic stalk and the eye. Defects in any of several transcription factors that control the development of the ventral retina and optic fissure can produce a coloboma (Gregory-Evans et al., 2004), including Vax1 and Vax2 (Barbieri et al., 2002; Mui et al., 2005), which are expressed in the ventral retina, and Pax2 (Favor et al., 1996), which is expressed along the optic fissure and around the optic disc. Signaling pathways implicated in the development of the ventral retina and optic disc include the hedgehog and BMP pathways (Take-uchi et al., 2003; Morcillo et al., 2006). Microphthalmia, coloboma and PFV are associated, either singly or in combination, with disruptions in retinoic acid signaling, resulting from vitamin A deficiency or excess (Wilson et al., 1953; Ozeki et al., 1999), mutations in the gene encoding retinaldehyde dehydrogenase 3 (Raldh3; Aldh1a3) (Dupé et al., 2003), or mutations in RAR and RXR receptors (Kastner et al., 1994; Kastner et al., 1997).

[1]Department of Molecular Biology and Genetics, [2]Department of Neuroscience, [3]Department of Ophthalmology, and the [4]Howard Hughes Medical Institute, Johns Hopkins University School of Medicine, Baltimore, MD 21205, USA.

*Author for correspondence (e-mail: jnathans@jhmi.edu)

Accepted 1 September 2008

The present study expands the set of signaling pathways relevant to these ocular defects by demonstrating that they can be caused by a deficiency in frizzled signaling. Integral membrane frizzled receptors, together with single-span Lrp5 and Lrp6 co-receptors, mediate canonical Wnt signaling (Gordon and Nusse, 2006). Planar cell polarity/tissue polarity signaling requires frizzled receptors, but appears to be independent of Lrp co-receptors and Wnt ligands. A third signaling pathway, the Wnt-calcium pathway, also utilizes frizzled receptors but is less well defined. In mammals there are ten frizzled (Fz; Fzd) genes, several of which are known to play important roles in development and/or human disease: *Fz3* controls axon guidance in the brain and spinal cord (Wang et al., 2002; Lyuksyutova et al., 2003; Wang et al., 2006a); *Fz4* controls vascular development in the retina and *FZ4* haploinsufficiency in humans is responsible for familial exudative vitreoretinopathy (FEVR) (Robataille et al., 2002; Xu et al., 2004); *Fz5* is required for yolk sac and placental angiogenesis and for survival of thalamic neurons in the parafasicular nucleus (Ishikawa et al., 2001; Liu et al., 2008); and *Fz6* controls the orientation of hair follicles and, together with *Fz3*, the orientation of a subset of inner-ear sensory hair cells as well as controlling neural tube closure (Guo et al., 2004; Wang et al., 2006b).

Thus far, the only connection between frizzled function and early ocular development has come from studies of *Fz5* in zebrafish and *Xenopus laevis* (Cavodeassi et al., 2005; Van Raay et al., 2005). In *Xenopus*, *Fz5* is expressed in the developing eye field where it promotes ocular cell fates. Later in development it is expressed in the optic cup, where it increases the proliferation of retinal progenitors and biases them towards adopting a neuronal rather than a glial fate. At present, the role of *Fz5* in mammalian ocular development remains largely unexplored. *Fz5*$^{-/-}$ mouse embryos die at embryonic day (E) 10, secondary to placental insufficiency (Ishikawa et al., 2001; Liu et al., 2008), precluding the use of these mice in the analysis of ocular development (Burns et al., 2008). In the present paper, we report the use of an *Fz5* conditional loss-of-function allele that bypasses the placental defect, thereby permitting a detailed analysis of ocular phenotypes from midgestation to adulthood. We observe a variety of defects in *Fz5*$^{-/-}$ mice, including microphthalmia, coloboma, PFV and a late retinal degeneration.

MATERIALS AND METHODS

Mice

Production, breeding and genotyping of *Fz5* mutant mice were as previously described (Liu et al., 2008).

Histochemistry and immunocytochemistry

Staining with 5-bromo-4-chloro-3-indolyl-β-D-galactopyranoside (X-Gal) or nitroblue tetrazolium/5-bromo-4-chloro-indolyl phosphate (NBT/BCIP) was performed with embryos, eyes or whole-mount retinas fixed in 4% paraformaldehyde (PFA) as described (Wang et al., 2002; Badea et al., 2003). Vibratome sections (200 μm) were prepared from X-Gal-stained E12.5 embryonic heads, and frozen sections (20 μm) were prepared from X-Gal-stained eyes. NBT/BCIP-stained adult retinas were sectioned at 20 μm to visualize single cells. For anti-Pax2 immunostaining and histologic analyses of the optic disc and fissure at E13.5, E14.5 and P1, horizontal sections were prepared from Carnoy's-fixed and wax-embedded heads. For anti-Pax2 and anti-Sox2 immunostaining of E10.5 embryos, freshly frozen coronal brain sections were used.

For immunocytochemistry or Hematoxylin and Eosin staining of adult retina, mice were perfused with 4% PFA, the retina was dissected and equilibrated with 30% sucrose, and frozen sections prepared. The following primary antibodies were used: rabbit anti-calretinin (1:500, Swant, 7669/4), mouse anti-Gfap (1:500, Sigma, G3893), rabbit anti-Gfap (1:500, ICN Biomedicals, 8451F), rabbit anti-glutamic acid decarboxylase (1:300, Chemicon, AB108), mouse anti-glutamine synthetase (1:100, Chemicon, MAB302), mouse anti-Islet1 (1:300, Developmental Studies Hybridoma Bank, 39.4D5), rabbit anti-synaptophysin (1:200, Sigma, S-5468) and rabbit anti-tyrosine hydroxylase (1:200, Chemicon, AB152).

For immunostaining of the whole-mount retina, the intact eye was fixed with 4% PFA for 20 minutes at room temperature, and then the retina was dissected, post-fixed with 4% PFA for 1 hour, washed with PBS, treated with RAPI buffer [150 mM NaCl, 1% NP40, 0.5% sodium deoxycholate, 0.1% SDS, 1 mM EDTA, 50 mM Tris (pH 8.0)] for 20 minutes, and incubated with one of the following primary antibodies at 4° C overnight: rabbit anti-neurofilament (1:500, Chemicon, AB1987), rabbit anti-Gfap (1:500, see above), FITC-conjugated mouse anti-smooth muscle actin (1:50, Sigma, F3777), or rabbit anti-Pax2 (1:200, Covance, PRB-276P). After incubation with primary and secondary antibodies, retinas were washed five times for 10 minutes each with PBST (0.1% Triton X-100 in PBS). Staining of the retinal vasculature with isolectin GS-IB4 (Molecular Probes, 1-21413) was performed as described (Xu et al., 2004).

In situ hybridization

RNA probe labeling and in situ hybridization were performed essentially as described (Rosen and Beddington, 1993). Briefly, E10.5 or E12.5 embryos were fixed and bisected at the midline, washed three times for 30 minutes each with RAPI buffer, post-fixed, washed with PBS, prehybridized and then hybridized overnight at 66°C. Post-hybridization steps were carried out as described (Rosen and Beddington, 1993). In situ probes were kindly provided by Dr Virginia E. Papaioannou of Columbia University (*Tbx5*), Dr Greg Lemke of the Salk Institute (*Vax2*) and Dr Gregg Duester of the Burnham Institute for Medical Research (*Raldh3*).

Plastic embedding and sectioning

Fixation, staining and embedding in Spurr's resin were performed as described (Soucy et al., 1998; Xu et al., 2004). To eliminate wrinkles, 0.5-μm semi-thin sections were floated on a droplet of 1:2 ethanol:water on a glass slide before heat drying and staining with Toluidine Blue.

Cell-death and cell-proliferation assays

To detect cell death, tissue sections or whole-mount embryos were stained with an antibody against cleaved caspase 3 (1:300, Cell Signaling, 9661) as described above. To detect cell proliferation, pregnant female mice received a 50 μg/g body weight intraperitoneal (IP) injection of BrdU at 10.5 days post-coitum. One hour after the injection, embryos were harvested, fixed with 4% PFA and embedded in paraffin. Sections were dewaxed, rehydrated, treated in 2M HCl for 20 minutes, and subjected to double immunostaining with antibodies against cleaved caspase 3 and BrdU (1:100 rat anti-BrdU, Abcam, AB6326).

Sparse labeling of Fz5 cells in the retina

4-Hydroxytamoxifen was introduced by IP injection into $Fz5^{CKO\text{-}AP/+}$;*R26-CreER* mice at 5 μg/g body weight, and the retinas processed as described (Badea et al., 2003).

Light-mediated damage

Light damage of the adult retina was performed as described (Rattner and Nathans, 2005).

Production of anti-Sox2 antibody

A DNA fragment encoding the C-terminal 168 amino acids of Sox2 was inserted into pGEMEX and pMAL expression vectors in order to prepare fusion proteins for production of immunogen and for affinity purification of the resulting antibodies, respectively. Rabbit anti-Sox2 antibodies were affinity purified from immunoblotted filter strips as described (Xiang et al., 1995).

RESULTS

Fz5 knock-in reporters reveal the pattern of expression of *Fz5* in the developing and adult retina

We recently described the production of two targeted alleles of the mouse *Fz5* gene: one in which the Fz5 coding region has been replaced with a β-galactosidase coding region to create a constitutive knockout allele ($Fz5^{lacZ}$); and a second in which a human placental alkaline phosphatase (AP) coding region has been inserted 3′ of a loxP-flanked *Fz5* coding region to create a conditional knockout allele ($Fz5^{CKO\text{-}AP}$) (Liu et al., 2008). Cre-mediated recombination of the $Fz5^{CKO\text{-}AP}$ allele leads to excision of the Fz5 coding region and expression of the AP coding region under the control of the *Fz5* promoter ($Fz5^{AP}$).

In most of the experiments described below we have used a *Sox2-Cre* transgene, which is expressed in embryonic but not extra-embryonic tissues, to provide Cre recombinase for gene inactivation. In embryos of genotype $Fz5^{CKO\text{-}AP/lacZ}$;*Sox2-Cre*, the restricted Cre expression bypasses the midgestational lethality associated with homozygous loss of *Fz5* in the placenta. In general, we have studied littermates from crosses that produced both control (e.g. $Fz5^{CKO\text{-}AP/+}$;*Sox2-Cre* or $Fz5^{lacZ/+}$;*Sox2-Cre*) and experimental (e.g. $Fz5^{CKO\text{-}AP/lacZ}$;*Sox2-Cre*) mice. We note that the formal genetic nomenclature, as written in the preceding sentence, defines the *Fz5* alleles prior to Cre-mediated recombination. For clarity, we will refer to $Fz5^{CKO\text{-}AP/+}$;*Sox2-Cre* as $Fz5^{+/-}$ and to $Fz5^{CKO\text{-}AP/lacZ}$;*Sox2-Cre* as $Fz5^{-/-}$, to indicate the actual tissue genotype that results from Cre-mediated recombination. With respect to the use of *Fz5* heterozygotes as controls, we have observed no differences between $Fz5^{+/-}$ and $Fz5^{+/+}$ mice and we therefore consider the phenotype of $Fz5^{+/-}$ to be representative of the wild type (WT).

Strong and relatively selective expression of *Fz5* in the developing mouse eye was noted in the initial description of the *Fz5* gene by in situ hybridization (Wang et al., 1996). By histochemical staining of embryos that are heterozygous for one of the reporter knock-in alleles described above (i.e. $Fz5^{lacZ/+}$ or $Fz5^{CKO\text{-}AP/+}$;*Sox2-Cre*), we observed that *Fz5* is specifically expressed in the developing eye field at E8.5, in the optic vesicle at E9.5, and in the optic cup and optic nerve at E12.5 (Fig. 1A-D). These observations are consistent with a recent in situ hybridization analysis of *Fz5* expression in mouse embryos (Burns et al., 2008). In the adult, X-Gal staining of $Fz5^{lacZ/+}$ retinas or AP staining of $Fz5^{CKO\text{-}AP/+}$;*Sox2-Cre* retinas results in contiguous deposition of the histochemical reaction product throughout all retinal layers (data not shown), a pattern that does not permit an analysis of the cell type(s) in which *Fz5* is expressed. To precisely define these cell types, we generated

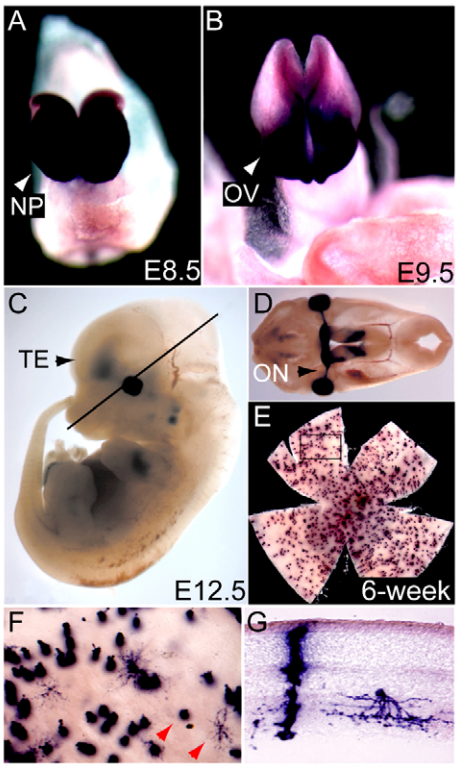

Fig. 1. Expression of *Fz5* in the embryonic eye field and adult retina. (**A**,**B**) Whole-mount *Fz5*$^{CKO\text{-}AP/+}$;*Sox2-Cre* mouse embryos stained with NBT/BCIP and viewed from the front. At E8.5, *Fz5* is expressed in the anterior neural plate (NP). At E9.5, *Fz5* expression is predominantly localized to the optic vesicles (OV). In B, the open cephalic neural tube can be seen above the zone of hybridization. (**C**,**D**) X-Gal-stained *Fz5*$^{lacZ/+}$ embryo at E12.5 showing *Fz5* expression in the ventral telencephalon (TE), eye and optic nerve (ON). D shows a vibratome section, the location of which is indicated by the line in C. (**E**,**F**) NBT/BCIP-stained flat-mount of a *Fz5*$^{CKO\text{-}AP/+}$;*R26-CreER* adult retina. Sparse labeling was achieved by low-dose 4-hydroxytamoxifen injection (see Materials and methods). The boxed region in E is shown enlarged in F. *Fz5* expression is restricted to Müller glia (left arrowhead) and to a subset of amacrine cells (right arrowhead). (**G**) A vertical section through the retina in E showing an AP-labeled Müller glial cell (left) and an amacrine cell (right). Here, and in all other retinal cross-sections, the outer nuclear layer is at the top of the image and the ganglion cell layer is at the bottom.

Fz5$^{CKO\text{-}AP/+}$;*R26-CreER* mice and treated them with a low dose of 4-hydroxytamoxifen to inefficiently activate the ubiquitously expressed Cre recombinase, thus generating a sparse distribution of *Fz5*$^{AP/+}$ cells (Badea et al., 2003). This analysis showed that in the adult retina, *Fz5* is expressed in Müller glia and amacrine cells (Fig. 1E-G).

Progressive retinal degeneration in the adult *Fz5*$^{-/-}$ eye

To determine whether *Fz5* plays a role in organizing the basic architecture of the retina, *Fz5*$^{+/-}$ and *Fz5*$^{-/-}$ retinas from mice at about postnatal day (P) 30 were immunostained for markers that are expressed in a variety of different retinal cell types, including calretinin (calbindin 2), Islet1 (Isl1), glutamic acid decarboxylase, tyrosine hydroxylase, synaptophysin, glutamine synthetase, and glial

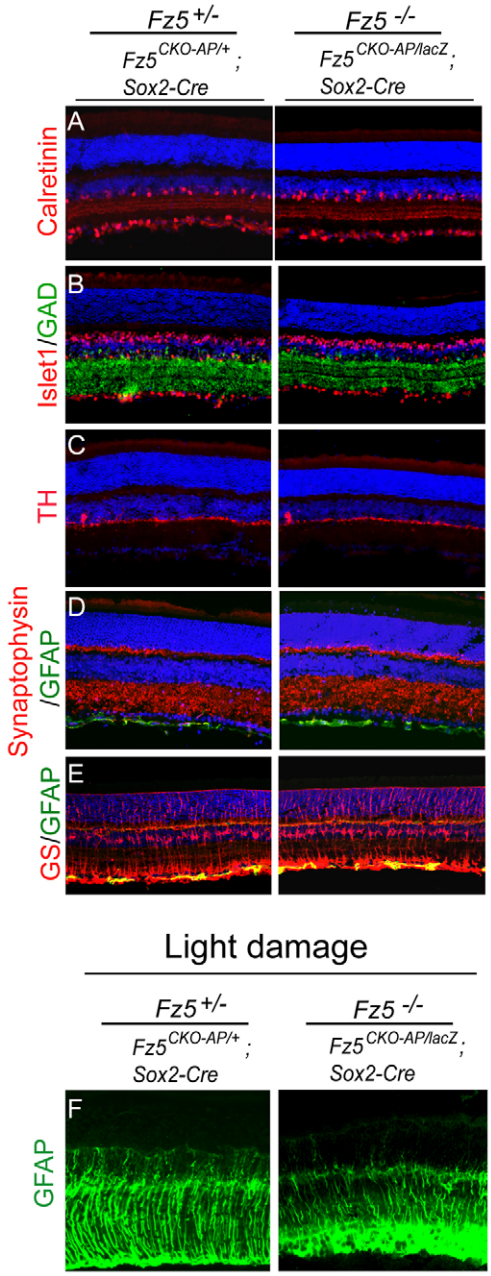

Fig. 2. The major cell types develop normally in the *Fz5*$^{-/-}$ retina at ~P30. (**A**) Amacrine cells, stained for calretinin, residing in the ganglion cell layer and inner nuclear layer show a characteristic trilamination of processes in the inner plexiform layer. (**B**) Nuclear localization of Islet1 in a subset of amacrine cells and retinal ganglion cells, and the distinctive inner plexiform layer stratification of processes of amacrine cells expressing glutamic acid decarboxylase (GAD). (**C**) Dopaminergic amacrine cells expressing tyrosine hydroxylase (TH) have processes that are confined to the outermost stratum of the inner plexiform layer. (**D**) Synaptophysin marks presynaptic terminals in the inner plexiform layer and outer plexiform layer, and glial fibrillary acidic protein (Gfap) marks astrocytes in the ganglion cell layer. (**E**) Glutamine synthetase (GS) in Müller glia and Gfap in astrocytes. (**F**) Similar extent of activation of Gfap expression in Müller glia of WT (*Fz5*$^{+/-}$) and *Fz5*$^{-/-}$ mouse retinas following exposure to bright light. Note that the intense Gfap immunoreactivity in the innermost region of the *Fz5*$^{-/-}$ retina is likely to reflect an excess of astrocytes (see Fig. 9). DAPI staining (blue) in A-E shows the three nuclear layers.

fibrillary acidic protein (Fig. 2A-E). In addition, *Fz5*$^{+/-}$ and *Fz5*$^{-/-}$ mice were subjected to 6 hours of bright light exposure with pupil dilation, a regimen that strongly induces glial fibrillary acidic protein (Gfap) expression in Müller glia in the WT retina (Fig. 2F). In each of these analyses, we observed no difference between *Fz5*$^{-/-}$ and WT retinas in the localization or abundance of molecular markers, retinal thickness, or in the number of DAPI-stained nuclei. Moreover, the optokinetic response to a visual stimulus, consisting of slowly moving black and white stripes, appeared normal in young adult *Fz5*$^{-/-}$ mice (Cahill and Nathans, 2008) (data not shown). Thus, in early adulthood, the loss of *Fz5* appears to have little effect on the overall structure of the retina or the response of Müller glia to retinal stress.

In contrast to the essentially normal appearance of *Fz5*$^{-/-}$ retinas in young adult mice, *Fz5*$^{-/-}$ retinas from mice that were more than 3-6 months old showed a variety of degenerative changes that progressively worsened with age. As shown in Fig. 3A,B, the degeneration included cell loss in all three retinal layers and a nearly complete loss of photoreceptor outer segments. Retinal folding and detachment typically accompanied the degeneration, together with an influx of macrophages or macrophage-like cells into the subretinal space (Fig. 3C-F). The retinal pigment epithelium remained grossly intact. At present, the molecular basis of this degenerative process is unknown but its pan-retinal character suggests that it arises from dysfunction of Müller glia.

Persistence of the fetal vasculature in the *Fz5*$^{-/-}$ eye

During fetal development, a rich vascular network develops within the vitreous and on the anterior and posterior surfaces of the developing lens (Goldberg, 1997). These vessels are normally eliminated before eye opening, a process that increases the optical clarity of the eye. The adult *Fz5*$^{-/-}$ vitreous differed from the WT in retaining a large vascular tree that enters the vitreous from the optic disc and ramifies and adheres to the posterior face of the lens (Fig. 4C-L). This vascular structure was invested with large numbers of pigmented cells (Fig. 4F,H,K), and its direct contiguity with the choroidal vasculature suggests that it is essentially an intra-ocular extension of the choroid (Fig. 4I-L). The persistent intravitreal vasculature was also invested with cells that express smooth muscle actin (Fig. 4D), suggesting that at least some of its component cells are of mesenchymal origin. Consistent with this idea, we observed an abnormally large number of cells between the lens and retina in the *Fz5*$^{-/-}$ eye at E14.5 (Fig. 4A,B), several days after periocular mesenchymal cells normally migrate through the ventral fissure and into the developing vitreous cavity. As described more fully below, the hypothesized increase in inward migration of periocular mesenchymal cells might be secondary to a delayed closure of the ventral fissure in the developing *Fz5*$^{-/-}$ eye.

Developmental defects in the ventral *Fz5*$^{-/-}$ eye and incomplete closure of the optic fissure

Upon external examination of *Fz5*$^{-/-}$ eyes, the most obvious ocular defects were microphthalmia and a tear-drop-shaped pupil due to a misshapen ventral iris border (Fig. 5E,F,I,J). To investigate the developmental origin of these anomalies, eyes from littermate *Fz5*$^{CKO\text{-}AP/lacZ}$*;Sox2-Cre* and *Fz5*$^{lacZ/+}$*;Sox2-Cre* embryos were X-Gal-stained and examined before and after sectioning (Fig. 5A-H). Microphthalmia was observed to begin as early as E10.5, and was accompanied by delayed and variable closure of the ventral fissure. The latter defect would be expected to retard development of the ventral zone of the iris and would account for the tear-drop-shaped pupil.

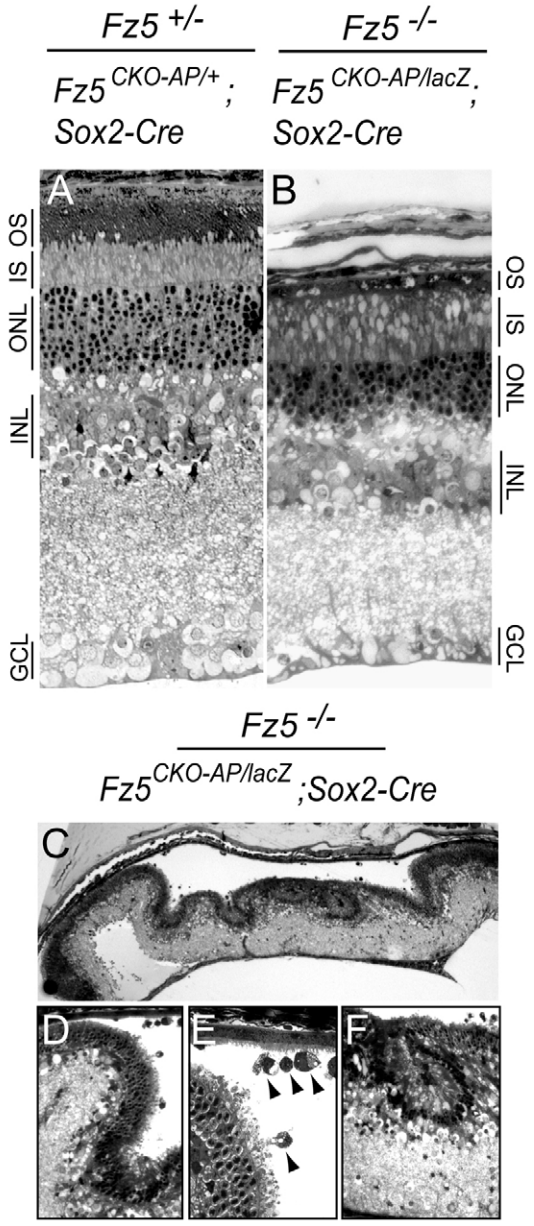

Fig. 3. Late degeneration of the *Fz5*$^{-/-}$ retina. (**A**,**B**) Semi-thin, plastic-embedded sections of (A) WT and (B) *Fz5*$^{-/-}$ mouse retinas at ~6 months of age stained with Toluidine Blue. In the *Fz5*$^{-/-}$ retina, there is a nearly complete loss of photoreceptor outer segments (OS), swelling of inner segments (IS), and cell and neuropil loss in the two plexiform and three nuclear layers (ONL, outer nuclear layer; INL, inner nuclear layer; GCL, ganglion cell layer). (**C**) *Fz5*$^{-/-}$ retina and choroid at ~6 months of age showing extensive retinal folding and detachment. (**D**,**F**) High-magnification views from C, showing detachment and folding (D) and rosette formation (F). (**E**) High-magnification view of the upper right corner of D showing that the subretinal space is populated by macrophages (arrowheads).

In the WT retina, the optic disc is both the only site towards which retinal ganglion cell axons are attracted and the only opening through which these axons pass out of the eye. In some *Fz5*$^{-/-}$ eyes, in which the retina was cleaved along the entire length of the ventral fissure, there was misrouting of a subset of retinal ganglion cell axon

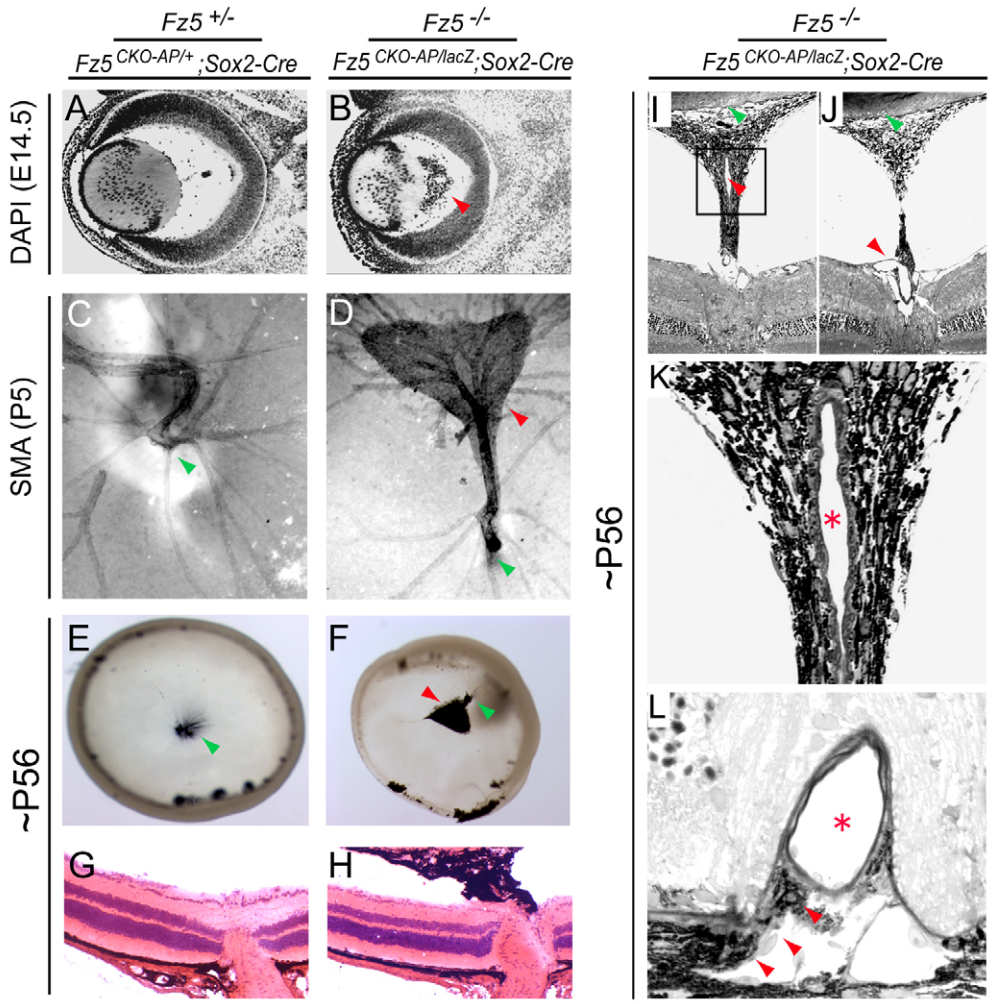

Fig. 4. Excess mesenchymal cells in the prenatal vitreous cavity and persistent fetal vasculature in the postnatal *Fz5*$^{-/-}$ eye. (**A**,**B**) DAPI-stained (A) WT and (B) *Fz5*$^{-/-}$ mouse embryonic eyes at E14.5. Arrowhead in B indicates the excess cells between the lens and retina. (**C**,**D**) Anti-smooth muscle actin (SMA) immunostaining of whole-mount retinas at P5. The hyaloid vessels and developing retinal vasculature emerge from the optic disk (green arrowheads). The cell mass that is attached to the optic disc in the *Fz5*$^{-/-}$ retina contains smooth muscle actin (D, red arrowhead). (**E-H**) Intact retinas viewed from the vitreal face (E,F) and Hematoxylin and Eosin-stained sections through the retina and optic nerve (G,H) at ~P56. The ectopic tissue (red arrowhead in F) is attached at the optic disc of the *Fz5*$^{-/-}$ retina (green arrowhead in F) and contains numerous pigment cells. (**I-L**) Semi-thin, plastic-embedded sections through the central retina showing the vascular structure and connectivity of the intra-vitreal tissue at ~P56. The serial sections at low magnification (I,J) show ectopic tissue attached to the optic disc (bottom) and the posterior face of the lens (top; green arrowheads). The large blood vessels in I and J are contiguous (red arrowheads). (K) High-magnification view of the boxed region in I, showing an intermingling of pigmented and unpigmented cells surrounding a large blood vessel (asterisk). (L) At the edge of the optic disc, pigmented cells associated with the initial segment of the intravitreal vasculature (asterisk) are contiguous with the pigmented cells of the choroid (arrowheads).

bundles, initially toward the ventral fissure and then secondarily toward the optic disc (Fig. 5K,L). This misrouting suggests that a persistently open ventral fissure resembles the optic disc in attracting growing axons.

As noted in the Introduction, several transcription factors and signaling pathways have been implicated in the development of the ventral retina and optic fissure. To test the integrity of these pathways, we examined the expression of the following markers: Raldh3 and Vax2, both of which are expressed in, and control the development of, the ventral retina; Tbx5, which is expressed in the dorsal retina; Pax2, which is expressed in the retina immediately adjacent to the optic disc; and Sox2, which is expressed in, and controls the proliferation of, retinal progenitors. Compared with the eyes of age-matched littermate controls, *Fz5*$^{-/-}$ eyes showed lower levels of *Raldh3*, *Vax2* and *Tbx5* transcripts, and a broader zone of Pax2 expression (Fig. 6). The pattern and intensity of Sox2 expression at E12.5 appeared essentially normal, although the entire *Fz5*$^{-/-}$ eye was already smaller at this stage.

To further explore the developmental basis of microphthalmia and the optic fissure defect, cell proliferation and cell death were analyzed by labeling with BrdU and by immunostaining for activated caspase 3, respectively. At E10.5, when the smaller size of the *Fz5*$^{-/-}$ eye is first apparent, the level of BrdU incorporation in *Fz5*$^{-/-}$ eyes was indistinguishable from that of the WT control, but was accompanied by a greater number of cells and cell fragments containing activated caspase 3 (Fig. 7E,F). The excess of activated caspase 3 was concentrated in the posterior/ventral eyecup, a region

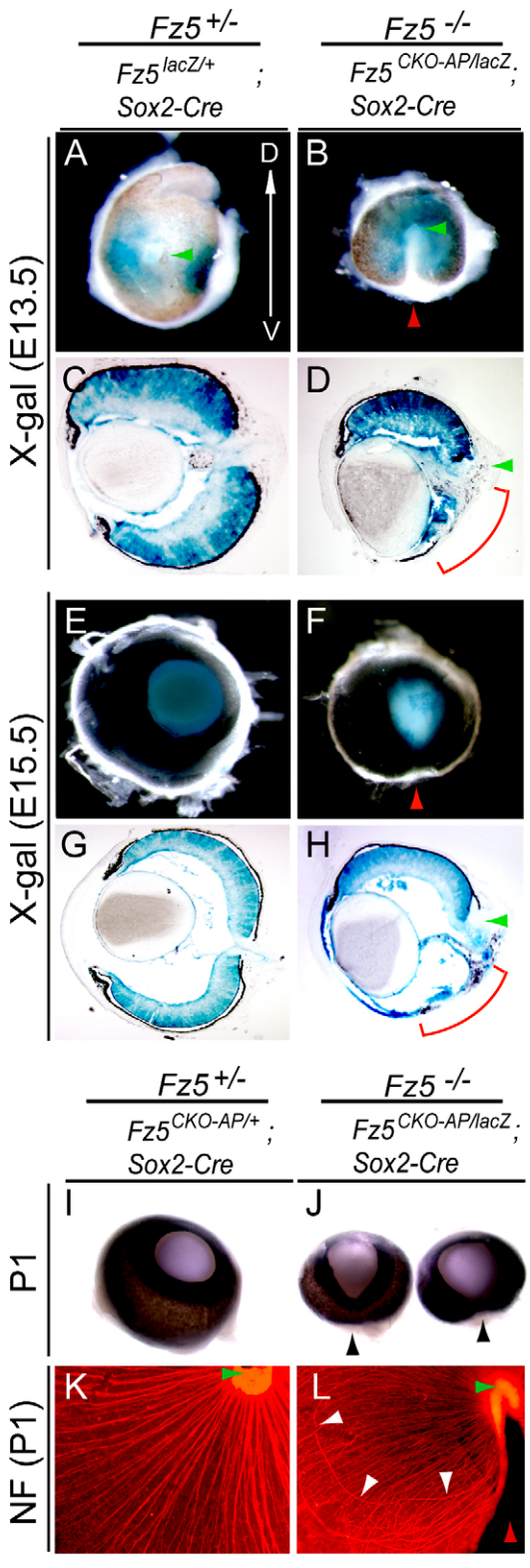

Fig. 5. Incomplete closure of the optic fissure in early retinal development produces a coloboma in the neonatal *Fz5*$^{-/-}$ eye. (**A**,**B**) X-Gal-stained whole-mounts of (A) *Fz5*$^{lacZ/+}$*;Sox2-CreER* (*Fz5*$^{+/-}$) and (B) *Fz5*$^{CKO-AP/lacZ}$*;Sox2-CreER* (*Fz5*$^{-/-}$) mouse eyes at E13.5 as viewed from the back, showing failed optic fissure closure in the *Fz5*$^{-/-}$ retina (red arrowheads). Green arrowheads indicate the optic nerve. (**C**,**D**) Vertical sections through the eyes shown in A,B. The red bracket in D (and H) demarcates the open ventral fissure. (**E**,**F**) Front view of X-Gal-stained eyes at E15.5. Note the tear-drop shape to the *Fz5*$^{-/-}$ iris. (**G**,**H**) Vertical sections through the eyes shown in E,F. (**I**,**J**) P1 eyes showing the typical *Fz5*$^{-/-}$ coloboma (arrowheads in J) and microphthalmia. (**K**,**L**) Anti-neurofilament (NF) immunostaining of whole-mount P1 retinas to visualize retinal ganglion cell axons. The optic disc is at the upper right (green arrowhead), and the open fissure is to the right in the *Fz5*$^{-/-}$ retina (red arrowhead). Misdirected bundles of retinal ganglion cell axons are seen in the *Fz5*$^{-/-}$ retina (white arrowheads). In all panels, dorsal is upward, as indicated in A (D, dorsal; V, ventral).

that normally has more cell death between E9 and E12 than other regions of the eyecup (Ozeki et al., 2000). Taken together, these data suggest that *Fz5* is required for the normal development and survival of early ocular progenitors in the ventral eyecup.

In the embryonic eye, Pax2 marks both the optic disc and the optic fissure (Otteson et al., 1998). In eyes sectioned in the horizontal plane, a narrow line of Pax2 staining was seen along the ventral retina at E13.5 in both WT and *Fz5*$^{-/-}$ embryos, with the only difference at this stage being a lateral expansion of the zone of Pax2 expression adjacent to the optic disc in the *Fz5*$^{-/-}$ eye (Fig. 8B,D). At E14.5, Pax2 expression in the ventral retina was extinguished in the WT eye, but persisted in the *Fz5*$^{-/-}$ eye (Fig. 8E-H).

An excess of astrocyte precursors and mature astrocytes in *Fz5*$^{-/-}$ eyes

Unlike retinal neurons and Müller glia, astrocytes are generated outside the retina and enter the eye by migrating along the optic nerve (Watanabe and Raff, 1988). In the late embryonic and early postnatal eye, Pax2-expressing astrocyte precursors are found both within the optic nerve and along the vitreal face of the retina (Otteson et al., 1998). Beginning in the early postnatal period, retinal astrocytes differentiate, start to express Gfap, and serve as a scaffold on which the retinal vasculature develops. WT and *Fz5*$^{-/-}$ retinas showed a similar distribution of Pax2-stained astrocyte precursors in the optic nerve at E14.5 (Fig. 8I-L). However, in the *Fz5*$^{-/-}$ eye at E16.5, the distribution of Pax2-stained cells near the optic nerve differed from that of the WT in that it extended along the adjacent ventral fissure region (Fig. 8M,N). This suggests that additional astrocyte precursors might be able to invade the *Fz5*$^{-/-}$ eye as a result of the delayed closure of the ventral fissure. Alternately, the Pax2-expressing cells that accumulate at the ventral fissure in the *Fz5*$^{-/-}$ eye could represent retinal cells that have been inappropriately converted into astrocyte precursors. Consistent with this latter interpretation, in the P1 *Fz5*$^{-/-}$ eye, there is a greater number and a more anterior distribution of astrocyte precursors relative to the WT control (Fig. 8O,P). Interestingly, the excess astrocytes persist in the early postnatal and adult *Fz5*$^{-/-}$ retina, but have little or no effect on intraretinal vascular development (Fig. 9).

DISCUSSION

In this paper, we have defined the ocular phenotypes associated with loss of *Fz5* in the mouse. The early phenotypes, listed in their order of appearance, are: increased cell death in the ventral retina, delayed and/or incomplete closure of the ventral fissure, an excess of mesenchymal cells in the vitreous cavity, an excess of retinal astrocyte precursors and mature astrocytes, and persistence of the

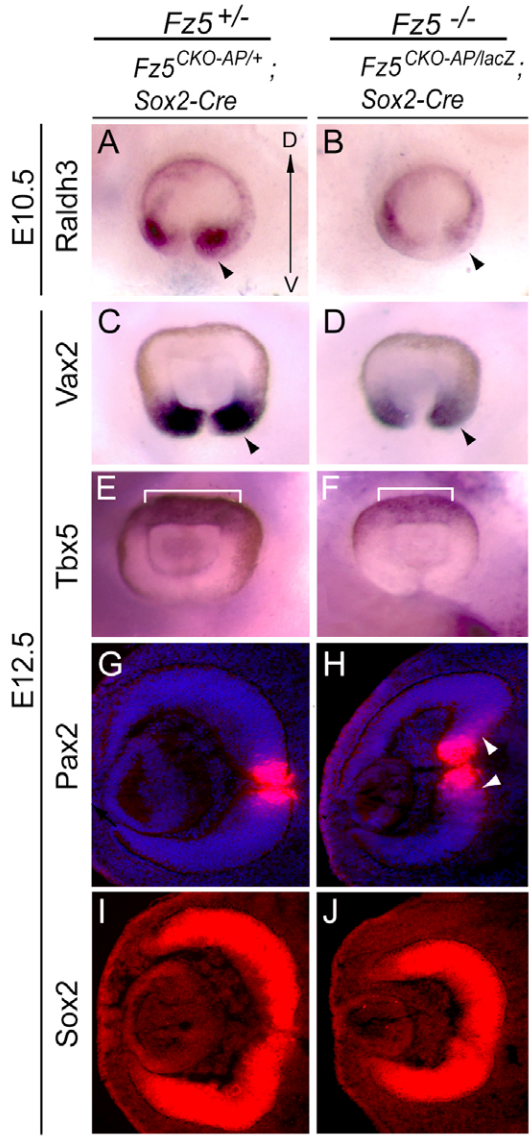

Fig. 6. Decreased expression of markers for ventral patterning during early *Fz5*$^{-/-}$ eye development. (**A-F**) The intact eye and surrounding tissue viewed from the cornea following whole-mount in situ hybridization. Dorsal is upward, as indicated in A. In the *Fz5*$^{-/-}$ mouse retina, ventral expression of *Raldh3* at E10.5 and of *Vax2* at E12.5 is decreased (arrowheads) whereas dorsal expression of *Tbx5* (bracket) is minimally affected. (**G**,**H**) At E12.5, immunolocalization of Pax2 in the *Fz5*$^{-/-}$ retina extends beyond the immediate vicinity of the optic disc (arrowheads). (**I**,**J**) The pan-retinal distribution of Sox2 immunostaining is similar in WT and *Fz5*$^{-/-}$ retinas at E12.5; note the smaller size of the *Fz5*$^{-/-}$ eye.

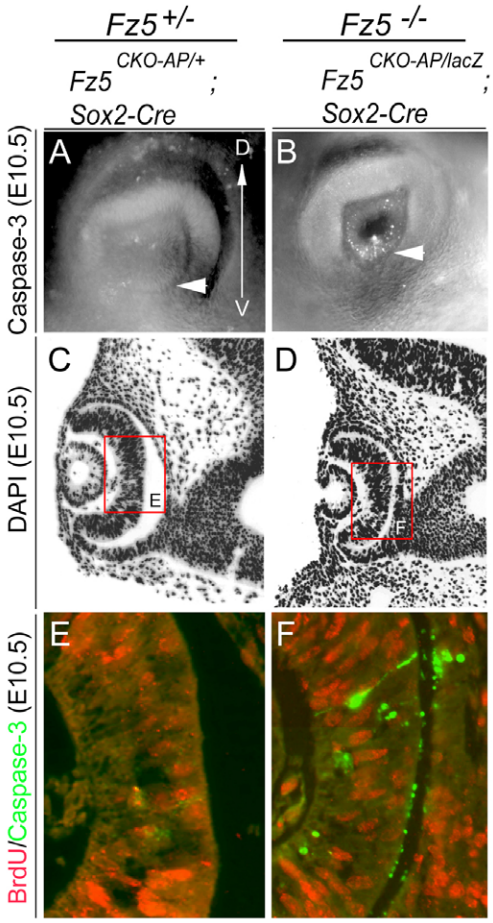

Fig. 7. Increased apoptosis in the *Fz5*$^{-/-}$ retina at E10.5. (**A**,**B**) Whole-mount mouse embryos immunostained for cleaved caspase 3 showing increased apoptosis in the ventral *Fz5*$^{-/-}$ optic cup (arrowhead). The intact optic cup is seen from the cornea. Dorsal is upward, as indicated in A. (**C-F**) Horizontal sections from littermate embryos harvested 1 hour after injection with BrdU. Sections were stained with DAPI (C,D) or immunostained for BrdU and activated caspase 3 (E,F). The boxed regions in C,D show the locations of E,F. In the *Fz5*$^{-/-}$ optic cup, many more cells and cell fragments in both the inner (future retina) and outer (future retinal pigment epithelium) layers contain activated caspase 3. Proliferation appears to be grossly normal in the *Fz5*$^{-/-}$ optic cup.

hyaloid vasculature in association with a large number of pigment cells. Despite these abnormalities and the resulting colobomatous and microphthalmic eye, the mature *Fz5*$^{-/-}$ retina appears essentially normal in early adulthood. A second phenotype, which we suspect is mechanistically unrelated to early eye development, consists of a late-onset, progressive and full-thickness retinal degeneration by ~6 months of age. Below, we discuss these findings in the context of previous work on frizzled signaling, early retinal development and congenital human ocular anomalies.

Fz5 signaling and mammalian eye development

The early *Fz5*$^{-/-}$ eye phenotype is similar to the phenotype seen in vitamin A-deprived rats and in *Raldh3*$^{-/-}$ mice (Wilson et al., 1953; Dupé et al., 2003). This similarity, together with the decreased expression of *Raldh3* in the E10.5 *Fz5*$^{-/-}$ retina, suggest that defects in retinoid signaling in the ventral retina might account, at least in part, for the *Fz5* phenotype. Decreased expression of Vax genes in the *Fz5*$^{-/-}$ E10.5 ventral retina is also a plausible mechanism by which the ventral fissure phenotype might arise, as *Vax1*$^{-/-}$ mice have a ventral fissure phenotype closely resembling that of *Fz5*$^{-/-}$ mice, *Vax2*$^{-/-}$ mice have a milder phenotype, and *Vax1*$^{-/-}$;*Vax2*$^{-/-}$ mice have a more severe phenotype (Barbieri et al., 2002; Mui et al., 2005). Finally, we note that Fz5 could act, at least in part, by altering Bmp7 signaling, which has been implicated in optic fissure formation (Morcillo et al., 2006), and/or by altering sonic hedgehog

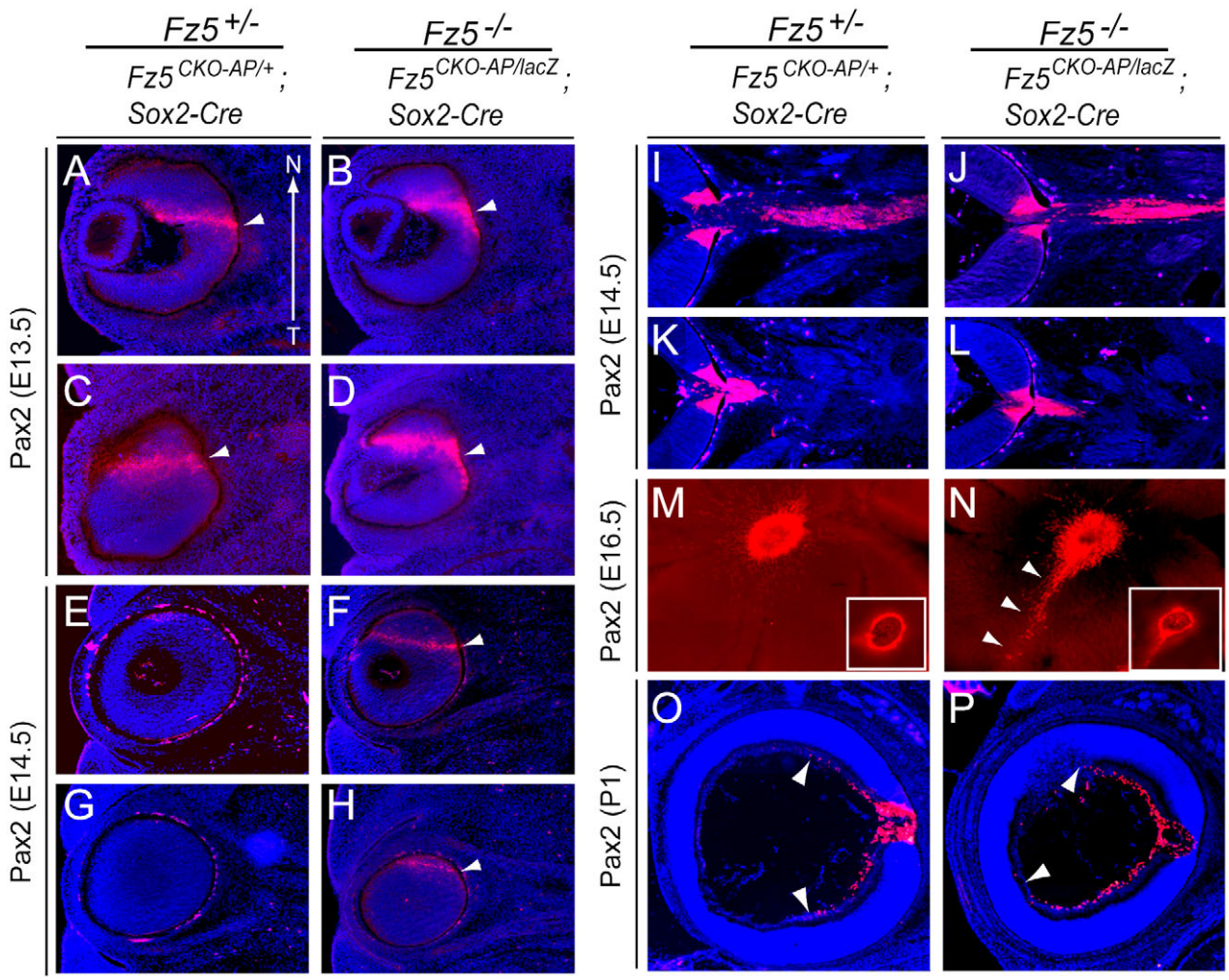

Fig. 8. Comparison of Pax2 immunolocalization during and after optic fissure closure in WT versus *Fz5*$^{-/-}$ retinas. In A-L, pairs of nearby sections are shown in order to better illustrate the staining and visualize the three-dimensional anatomy. (**A-D**) Anti-Pax2 immunostaining at E13.5 showing the posterior expansion of the domain of Pax2 expression in the *Fz5*$^{-/-}$ optic fissure. Arrowheads indicate the posterior border of the optic fissure and the zone of Pax2 expression that tracks the optic fissure. (**E-H**) At E14.5, when Pax2 is no longer detected in the ventral retina in the WT mouse, it continues to mark the ventral fissure in the *Fz5*$^{-/-}$ retina. A-H are sectioned in the horizontal plane; nasal is upward, as indicated in A (N, nasal; T, temporal). (**I-L**) At E14.5, Pax2 abundance in the optic disc and optic nerve is similar in WT and *Fz5*$^{-/-}$ retinas. (**M**,**N**) Whole-mount immunostaining at E16.5 showing Pax2 in the ventral fissure region of the *Fz5*$^{-/-}$ retina. Insets show a plane of focus within the optic disc, showing a ring of Pax2-positive cells around the optic nerve. (**O**,**P**) The number and lateral distribution of Pax2-expressing astrocyte precursors at the vitreal face of the retina are increased in the *Fz5*$^{-/-}$ eye.

signaling, which has been implicated in optic disc and optic stalk development and in the proliferation of optic nerve astrocytes (Wallace and Raff, 1999; Dakubo et al., 2003).

Fz5 has also been implicated in early eye development in zebrafish and *Xenopus* (Cavodeassi et al., 2005; Van Raay et al., 2005). Interestingly, our observations of normal levels of *Sox2* expression in the embryonic *Fz5*$^{-/-}$ retina and a normal density of Müller glia and of multiple neuronal cell types within the mature *Fz5*$^{-/-}$ retina, differ from the results obtained in *Xenopus* by Van Raay et al. (Van Raay et al., 2005). In *Xenopus*, Fz5 was proposed to function via Sox2 to promote the proliferation of retinal progenitors and their acquisition of neural rather than Müller glial cell fates. Although the major glia in the retina, Müller cells and astrocytes, have different origins – the former developing from retinal progenitors and the latter migrating into the retina from the optic disc – it is intriguing that the only major alterations in cell number in *Fz5*-deficient mouse and *Xenopus* eyes are, respectively, an increase in astrocytes and Müller glia. Taken together, these two sets of observations suggest that mammals and amphibians have evolved different pathways through which Fz5 signaling controls early eye development, and/or different degrees to which Fz5 signaling impinges on each of several common pathways.

The full-thickness retinal degeneration seen in *Fz5*$^{-/-}$ mice is striking for its late onset, and is reminiscent of the late onset of the *Fz5*$^{-/-}$ phenotype of progressive neuronal loss in the parafasicular nucleus of the thalamus (Liu et al., 2008). In both the thalamus and retina, proliferation, migration and terminal differentiation of *Fz5*$^{-/-}$ cells proceed normally and cell loss is not observed until weeks (in the thalamus) or months (in the retina) later. In the thalamus, timed deletion of a conditional *Fz5* allele using 4-hydroxytamoxifen and *R26-CreER* further demonstrated a continuous requirement for *Fz5* signaling to maintain neuronal viability. Since *Fz5* expression is restricted to Müller glia and amacrine cells in the mature retina, the retinal degeneration in *Fz5*$^{-/-}$ mice might reflect a progressive

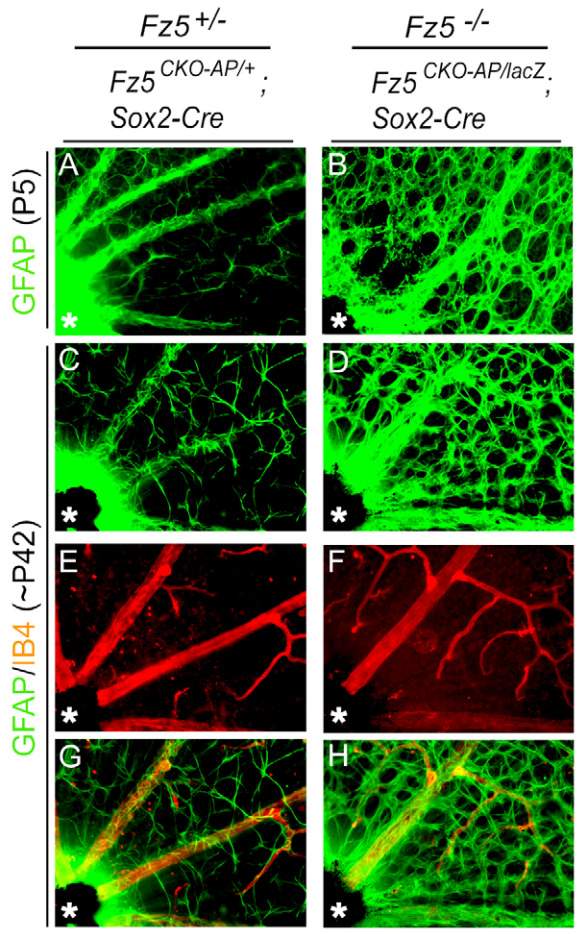

Fig. 9. An increase in the number of astrocytes in the *Fz5*$^{-/-}$ retina. (**A**,**B**) Flat-mount mouse retinas at P5 immunostained for Gfap to visualize astrocytes. The optic disc is at the lower left in all panels (asterisk). (**C-H**) Flat-mount retinas at ~P42 showing astrocytes (Gfap) and the vasculature (lectin IB4) on the inner face of the retina. Merged images from C-F are shown in G,H. At ~P42, the retinal vasculature appears normal. At both ages (P5 and ~P42), the *Fz5*$^{-/-}$ retina has an increased density of astrocytes compared with the WT.

dysfunction or loss of Müller glia secondary to a requirement for ongoing Fz5 signaling, with neuronal loss beginning only after a threshold has been reached in Müller cell dysfunction.

Implications for human ocular malformation and retinal degeneration

In humans, ocular coloboma is a relatively common congenital malformation, with an incidence of ~1.4 per 10,000 births in Western Europe (Stoll et al., 1997; Morrison et al., 2002). Coloboma is associated with over 20 Mendelian syndromes, as well as with various chromosomal anomalies and alterations at many unmapped loci (Gregory-Evans et al., 2004). Among the siblings of affected individuals, the incidence of coloboma is ~100-fold higher than in the general population (Morrison et al., 2002), and it is also more common among progeny of consanguineous unions (Hornby et al., 2003). Additionally, vitamin A deficiency during gestation has been implicated as an environmental risk factor for coloboma (Seeliger et al., 1999; Hornby et al., 2002), consistent with the effect of vitamin A deficiency in rats and with the phenotypes of mice with targeted disruptions in genes involved in retinoic acid signaling. Microphthalmia has an incidence of ~1 per 10,000 births in the United States and Western Europe (Stoll et al., 1997; Källén et al., 1996; Källén and Tornqvist, 2005), and alcohol exposure during gestation is a major environmental risk factor for microphthalmia, making microphthalmia one of the classic stigmata of fetal alcohol syndrome. As of June 2008, Online Mendelian Inheritance in Man (OMIM; http://www.ncbi.nlm.nih.gov/sites/entrez?db=omim) listed 82 entries for coloboma, 82 for microphthalmia, and 25 for both defects.

The incidence of PFV is unknown, although it has been described as one of the most common developmental anomalies in the human eye (Duke-Elder, 1964). In the general population, small and generally innocuous remnants of the intraocular vasculature are often observed ophthalmoscopically on the posterior surface of the lens (‘Mittendorf’s dot’) and on the optic disc (‘Bergmeister’s papilla’) (Goldberg, 1997).

Thus far, genes involved in Wnt/frizzled signaling have not been implicated in late retinal degeneration, coloboma or microphthalmia in humans, and Wnt/frizzled signaling has only been indirectly implicated in one subtype of PFV. In subjects with Norrie disease or with osteoporosis-pseudoglioma syndrome, the absence of Norrin (NDP)-mediated activation of FZ4 and its co-receptor, LRP5, blocks the development of the intraretinal vasculature, which indirectly inhibits the regression of the adjacent fetal vasculature in the vitreous (Berger and Ropers, 2001; Gong et al., 2001; Xu et al., 2004). The present work strongly suggests that FZ5, as well as intracellular and extracellular components of Wnt signal transduction that are expressed in early eye development, are relevant to genetic or combined genetic/environmental susceptibilities to retinal degeneration, microphthalmia, coloboma and PFV in humans.

We thank Hugh Cahill for performing optokinetic testing; Tudor Badea, Seth Blackshaw, Morton Goldberg and Amir Rattner for advice, assistance or reagents; and Tudor Badea and Xin Ye for helpful comments on the manuscript. This work was supported by The National Eye Institute (NIH) and the Howard Hughes Medical Institute.

References

Badea, T., Wang, Y. and Nathans, J. (2003). A noninvasive genetic/pharmacologic strategy for visualizing cell morphology and clonal relationships in the mouse. *J. Neurosci.* **23**, 2314-2322.

Barbieri, A. M., Broccoli, V., Bovolenta, P., Alfano, G., Marchitiello, A., Mocchetti, C., Crippa, L., Bulfone, A., Marigo, V., Ballabio, A. et al. (2002). Vax2 inactivation in mouse determines alteration of the eye dorsal-ventral axis, misrouting of the optic fibres and eye coloboma. *Development* **129**, 805-813.

Berger, W. and Ropers, H. H. (2001). Norrie disease. In *The Metabolic and Molecular Basis of Inherited Disease* 8th edn (ed. C. R. Scriver, A. L. Beaudet, W. S. Sly and D. Valle), pp. 5977-5985. New York, NY: McGraw-Hill.

Burns, C. J., Zhang, J., Brown, E. C., Van Bibber, A. M., Van Es, J., Clevers, H., Ishikawa, T. O., Taketo, M. M., Vetter, M. L. and Fuhrmann, S. (2008). Investigation of Frizzled-5 during embryonic neural development in mouse. *Dev. Dyn.* **237**, 1614-1626.

Cahill, H. and Nathans, J. (2008). The optokinetic reflex as a tool for quantitative analyses of nervous system function in mice: application to genetic and drug-induced variation. *PLOS One* **3**, e2055.

Cavodeassi, F., Carreira-Barbosa, F., Young, R. M., Concha, M. L., Allende, M. L., Houart, C., Tada, M. and Wilson, S. W. (2005). Early stages of zebrafish eye formation require the coordinated activity of Wnt11, Fz5, and the Wnt/beta-catenin pathway. *Neuron* **47**, 43-56.

Dakubo, G. D., Wang, Y. P., Mazerolle, C., Campsall, K., McMahon, A. P. and Wallace, V. A. (2003). Retinal ganglion cell-derived sonic hedgehog signaling is required for optic disc and stalk neuroepithelial cell development. *Development* **130**, 2967-2980.

Duke-Elder, S. (1964). *System of Ophthalmology: Normal and Abnormal Development*, pp. 764-770. St Louis, MO: C. V. Mosby.

Dupé, V., Matt, N., Garnier, J. M., Chambon, P., Mark, M. and Ghyselinck, N. B. (2003). A newborn lethal defect due to inactivation of retinaldehyde dehydrogenase type 3 is prevented by maternal retinoic acid treatment. *Proc. Natl. Acad. Sci. USA* **100**, 14036-14041.

Favor, J., Sandulache, R., Neuhäuser-Klaus, A., Pretsch, W., Chatterjee, B., Senft, E., Wurst, W., Blanquet, V., Grimes, P., Spörle, R. et al. (1996). The mouse Pax2(1Neu) mutation is identical to a human PAX2 mutation in a family with renal-coloboma syndrome and results in developmental defects of the brain, ear, eye, and kidney. *Proc. Natl. Acad. Sci. USA* **93**, 13870-13875.
Goldberg, M. F. (1997). Persistent fetal vasculature (PFV): an integrated interpretation of signs and symptoms associated with persistent hyperplastic primary vitreous (PHPV). LIV Edward Jackson Memorial Lecture. *Am. J. Ophthalmol.* **124**, 587-626.
Gong, Y., Slee, R. B., Fukai, N., Rawadi, G., Roman-Roman, S., Reginato, A. M., Wang, H., Cundy, T., Glorieux, F. H., Lev, D. et al. (2001). Osteoporosis-Pseudoglioma Syndrome: LDL receptor-related protein 5 (LRP5) affects bone accrual and eye development. *Cell* **107**, 513-523.
Gordon, M. D. and Nusse, R. (2006). Wnt signaling: multiple pathways, multiple receptors, and multiple transcription factors. *J. Biol. Chem.* **281**, 22429-22433.
Gregory-Evans, C. Y., Williams, M. J., Halford, S. and Gregory-Evans, K. (2004). Ocular coloboma: a reassessment in the age of molecular neuroscience. *J. Med. Genet.* **41**, 881-891.
Guo, N., Hawkins, C. and Nathans, J. (2004). Frizzled6 controls hair patterning in mice. *Proc. Natl. Acad. Sci. USA* **101**, 9277-9281.
Hornby, S. J., Ward, S. J., Gilbert, C. E., Dandona, L., Foster, A. and Jones, R. B. (2002). Environmental risk factors in congenital malformations of the eye. *Ann. Trop. Paediatr.* **22**, 67-77.
Hornby, S. J., Dandona, L., Jones, R. B., Stewart, H. and Gilbert, C. E. (2003). The familial contribution to non-syndromic ocular coloboma in south India. *Br. J. Ophthalmol.* **87**, 336-340.
Horsford, D. J., Hanson, I., Freund, C., McInnes, R. R. and van Heyningen, V. (2001). Transcription factors in eye disease and ocular development. In *The Metabolic and Molecular Basis of Inherited Disease*, 8th edn (ed. C. R. Scriver, A. L. Beaudet, W. S. Sly and D. Valle), pp. 5987-6032. New York, NY: McGraw-Hill.
Ishikawa, T., Tamai, Y., Zorn, A. M., Yoshida, H., Seldin, M. F., Nishikawa, S. and Taketo, M. M. (2001). Mouse Wnt receptor gene Fzd5 is essential for yolk sac and placental angiogenesis. *Development* **128**, 25-33.
Källén, B. and Tornqvist, K. (2005). The epidemiology of anophthalmia and microphthalmia in Sweden. *Eur. J. Epidemiol.* **20**, 345-350.
Källén, B., Robert, E. and Harris, J. (1996). The descriptive epidemiology of anophthalmia and microphthalmia. *Int. J. Epidemiol.* **25**, 1009-1016.
Kastner, P., Grondona, J. M., Mark, M., Gansmuller, A., LeMeur, M., Decimo, D., Vonesch, J. L., Dollé, P. and Chambon, P. (1994). Genetic analysis of RXR alpha developmental function: convergence of RXR and RAR signaling pathways in heart and eye morphogenesis. *Cell* **78**, 987-1003.
Kastner, P., Mark, M., Ghyselinck, N., Krezel, W., Dupé, V., Grondona, J. M. and Chambon, P. (1997). Genetic evidence that the retinoid signal is transduced by heterodimeric RXR/RAR functional units during mouse development. *Development* **124**, 313-326.
Liu, C., Wang, Y., Smallwood, P. M. and Nathans, J. (2008). An essential role for Frizzled5 in neuronal survival in the parafascicular nucleus of the thalamus. *J. Neurosci.* **28**, 5641-5653.
Lyuksyutova, A. I., Lu, C. C., Milanesio, N., King, L. A., Guo, N., Wang, Y., Nathans, J., Tessier-Lavigne, M. and Zou, Y. (2003). Anterior-posterior guidance of commissural axons by Wnt-frizzled signaling. *Science* **302**, 1984-1988.
Morcillo, J., Martínez-Morales, J. R., Trousse, F., Fermin, Y., Sowden, J. C. and Bovolenta, P. (2006). Proper patterning of the optic fissure requires the sequential activity of BMP7 and SHH. *Development* **133**, 3179-3190.
Morrison, D., FitzPatrick, D., Hanson, I., Williamson, K., van Heyningen, V., Fleck, B., Jones, I., Chalmers, J. and Campbell, H. (2002). National study of microphthalmia, anophthalmia, and coloboma (MAC) in Scotland: investigation of genetic aetiology. *J. Med. Genet.* **39**, 16-22.
Mui, S. H., Kim, J. W., Lemke, G. and Bertuzzi, S. (2005). Vax genes ventralize the embryonic eye. *Genes Dev.* **19**, 1249-1259.
Otteson, D. C., Shelden, E., Jones, J. M., Kameoka, J. and Hitchcock, P. F. (1998). Pax2 expression and retinal morphogenesis in the normal and Krd mouse. *Dev. Biol.* **193**, 209-224.
Ozeki, H., Shirai, S., Ikeda, K. and Ogura, Y. (1999). Critical period for retinoic acid-induced developmental abnormalities of the vitreous in mouse fetuses. *Exp. Eye Res.* **68**, 223-228.
Ozeki, H., Ogura, Y., Hirabayashi, Y. and Shimada, S. (2000). Apoptosis is associated with formation and persistence of the embryonic fissure. *Curr. Eye Res.* **20**, 367-372.
Rattner, A. and Nathans, J. (2005). The genomic response to retinal disease and injury: evidence for endothelin signaling from photoreceptors to glia. *J. Neurosci.* **25**, 4540-4549.
Robitaille, J., MacDonald, M. L., Kaykas, A., Sheldahl, L. C., Zeisler, J., Dubé, M. P., Zhang, L. H., Singaraja, R. R., Guernsey, D. L., Zheng, B. et al. (2002). Mutant frizzled-4 disrupts retinal angiogenesis in familial exudative vitreoretinopathy. *Nat. Genet.* **32**, 326-330.
Rosen, B. and Beddington, R. S. (1993). Whole-mount in situ hybridization in the mouse embryo: gene expression in three dimensions. *Trends Genet.* **9**, 162-167.
Seeliger, M. W., Biesalski, H. K., Wissinger, B., Gollnick, H., Gielen, S., Frank, J., Beck, S. and Zrenner, E. (1999). Phenotype in retinol deficiency due to a hereditary defect in retinol binding protein synthesis. *Invest. Ophthalmol. Vis. Sci.* **40**, 3-11.
Soucy, E., Wang, Y., Nirenberg, S., Nathans, J. and Meister, M. (1998). A novel signaling pathway from rod photoreceptors to ganglion cells in mammalian retina. *Neuron* **21**, 481-493.
Stoll, C., Alembik, Y., Dott, B. and Roth, M. P. (1997). Congenital eye malformations in 212,479 consecutive births. *Ann. Genet.* **40**,122-128.
Take-uchi, M., Clarke, J. D. and Wilson, S. W. (2003). Hedgehog signalling maintains the optic stalk-retinal interface through the regulation of Vax gene activity. *Development* **130**, 955-968.
Van Raay, T. J., Moore, K. B., Iordanova, I., Steele, M., Jamrich, M., Harris, W. A. and Vetter, M. L. (2005). Frizzled 5 signaling governs the neural potential of progenitors in the developing Xenopus retina. *Neuron* **46**, 23-36.
Verma, A. S. and Fitzpatrick, D. R. (2007). Anophthalmia and microphthalmia. *Orphanet. J. Rare Dis.* **2**, 47.
Wallace, V. A. and Raff, M. C. (1999). A role for Sonic hedgehog in axon-to-astrocyte signalling in the rodent optic nerve. *Development* **126**, 2901-2909.
Wang, Y., Macke, J. P., Abella, B. S., Andreasson, K., Worley, P., Gilbert, D. J., Copeland, N. G., Jenkins, N. A. and Nathans, J. (1996). A large family of putative transmembrane receptors homologous to the product of the Drosophila tissue polarity gene frizzled. *J. Biol. Chem.* **271**, 4468-4476.
Wang, Y., Thekdi, N., Smallwood, P. M., Macke, J. P. and Nathans, J. (2002). Frizzled-3 is required for the development of major fiber tracts in the rostral CNS. *J. Neurosci.* **22**, 8563-8573.
Wang, Y., Zhang, J., Mori, S. and Nathans, J. (2006a). Axonal growth and guidance defects in Frizzled3 knock-out mice: a comparison of diffusion tensor magnetic resonance imaging, neurofilament staining, and genetically directed cell labeling. *J. Neurosci.* **26**, 355-364.
Wang, Y., Guo, N. and Nathans, J. (2006b). The role of Frizzled3 and Frizzled6 in neural tube closure and in the planar polarity of inner-ear sensory hair cells. *J. Neurosci.* **26**, 2147-2156.
Watanabe, T. and Raff, M. C. (1998). Retinal astrocytes are immigrants from the optic nerve. *Nature* **332**, 834-837.
Wilson, J. G., Roth, C. B. and Warkay, J. (1953). An analysis of the syndrome of malformations induced by maternal vitamin A deficiency: effects of restoration of vitamin A at various times during gestation. *Am. J. Anat.* **92**, 189-217.
Xiang, M., Zhou, L., Macke, J. P., Yoshioka, T., Hendry, S. H. C., Eddy, R. L., Shows, T. B. and Nathans, J. (1995). The Brn-3 family of POU-domain factors: primary structure, binding specificity, and expression in subsets of retinal ganglion cells and somatosensory neurons. *J. Neurosci.* **15**, 4762-4785.
Xu, Q., Wang, Y., Dabdoub, A., Smallwood, P. M., Williams, J., Woods, C., Kelley, M. W., Jiang, L., Tasman, W., Zhang, K. et al. (2004). Vascular development in the retina and inner ear: control by Norrin and Frizzled-4, a high-affinity ligand-receptor pair. *Cell* **116**, 883-895.